A G protein/cAMP signal cascade is required for axonal convergence into olfactory glomeruli

Alexander T. Chesler, Dong-Jing Zou, Claire E. Le Pichon, Zita A. Peterlin, Glennis A. Matthews, Xin Pei, Michael C. Miller, and Stuart Firestein†

Department of Biological Sciences, Columbia University, 1212 Amsterdam Avenue, New York, NY 10027

Edited by Linda M. Bartoshuk, Yale University School of Medicine, New Haven, CT, and approved November 7, 2006 (received for review October 20, 2006)

The mammalian odorant receptors (ORs) comprise a large family of G protein-coupled receptors that are critical determinants of both the odorant response profile and the axonal identity of the olfactory sensory neurons in which they are expressed. Although the pathway by which ORs activate odor transduction is well established, the mechanism by which they direct axons into proper glomerular relationships remains unknown. We have developed a gain-of-function approach by using injection of retroviral vectors into the embryonic olfactory epithelium to study the ORs' contribution to axon guidance. By ectopically expressing ORs, we demonstrate that functional OR proteins induce axonal coalescence. Furthermore, ectopic expression of Gα mutants reveals that activation of the signal transduction cascade is sufficient to cause axonal convergence into glomeruli. Analysis of Gα subunit expression indicates that development and odorant transduction use separate transduction pathways. Last, we establish that the generation of cAMP through adenylyl cyclase 3 is necessary to establish proper axonal identity. Our data point to a model in which axonal sorting is accomplished by OR stimulation of cAMP production by coupling to Gαs.

axon guidance | development | olfaction

In mammalian olfactory systems, axons from olfactory sensory neurons (OSNs) in the olfactory epithelium (OE) project to the olfactory bulb (OB), where they coalesce into glomeruli. Strikingly, any given glomerulus is populated exclusively by axons of cells expressing the same odorant receptor (OR) (1, 2). This feat is all the more remarkable because, with ≈1,000 ORs in mouse (3, 4) and each neuron expressing only one of those receptors (5), there are effectively >1,000 populations of neurons that must properly sort. Although the glomerulus is believed to be a functional unit of odor coding, surprisingly little is known of the factors critical to its formation.

Genetic lesions of a cyclic nucleotide-gated channel subunit CNGA2 (6–8) or a G protein subunit Gαolf (9) effectively silence the odor response but do not appear to severely affect the organization of glomeruli in neonates. On the other hand, even minor changes in the OR protein cause shifts in glomerular position (10). There are two distinct processes at work: coalescence of like axons into a glomerulus and determination of a specific position for that glomerulus. Since the initial finding a decade ago that ORs are critical determinants in OSN axonal convergence (1), there has been little further insight into the mechanisms of glomerular formation. Many factors have been implicated in glomerular positioning (11) but not directly in the coalescence of axons into specific glomeruli. In the absence of projection neurons, interneurons, or even much of the OB itself, axons from OSNs expressing OR P2 still coalesce (11). This result has led to the notion that glomerular coalescence does not require a preexisting "target," is intrinsic to OSN axons, and is mediated by the ORs themselves (10).

However, there is mounting evidence that activity-generated processes might affect glomerular formation. We recently found that the mature organization of the olfactory system cannot occur in the absence of cellular activity (12). Similarly, in adenylyl cyclase type 3 (AC3) knockout mice, glomerular structure is highly perturbed (13, 14). Furthermore, both spontaneous and synaptic activity seem to be essential for the establishment and maintenance of proper connectivity (15).

Thus, in contrast to the visual system in which patterned activity plays a clear role in the establishment of precise projections, there are conflicting data concerning the effect of activity on glomerular development. Here we address the possibility that a critical feature of activity in the olfactory system is the production of cAMP by activation of the G protein cascade. Such a model would explain why CNGA2 knockout mice, which retain G protein signaling despite odor-evoked electrical silence, achieve largely normal glomerular formation, but AC3 knockout mice do not. Why then do knockouts of Gαolf, which couples ORs to AC3 in mature OSNs, also appear to have normal glomeruli for OR P2 at birth (9)? Here we show that an alternative G protein, Gαs, likely fulfills this essential role during development. The direct involvement of G protein/cAMP signaling in the formation of olfactory projections provides a mechanism in the formation of sensory maps.

Results

***In Utero* Imaging and Injection of the Developing Olfactory System.** We have developed the use of retroviral vectors as an alternative approach to transgenic mice for studying the molecular genetics of mammalian olfactory development *in vivo*. To deal with the small target size of the embryonic olfactory system, we modified previously published protocols for imaging embryonic ventricles with an ultrasound biomicroscope (16). We constructed a retroviral vector encoding tauGFP (tGFP) that, when injected into the embryonic OE, was expressed robustly in the developing OE and persisted into adulthood. Examination of postnatal day 21 (P21) mice injected with the tGFP retroviral vector at embryonic day 11 (E11) revealed widespread ectopic expression specifically throughout the OE (Fig. 1*A*). We had similar success injecting at various stages (E10.5–E16) and also extended our study to rats (E13–E18).

Injection of the retroviral vector resulted in numerous clusters of $tGFP^+$ cells composed of multiple cell types, including basal cells, OSNs, and apical sustentacular cells (data not shown). In addition to labeling cell bodies in the OE, tGFP-labeled axons of

Author contributions: A.T.C. and D-J.Z. contributed equally to this work; A.T.C., D-J.Z., and S.F. designed research; A.T.C., D-J.Z., C.E.L.P., Z.A.P., G.A.M., X.P., and M.C.M. performed research; A.T.C., D-J.Z., C.E.L.P., Z.A.P., and G.A.M. contributed new reagents/analytic tools; A.T.C., D-J.Z., C.E.L.P., Z.A.P., and X.P. analyzed data; and A.T.C., D-J.Z., and S.F. wrote the paper.

The authors declare no conflict of interest.

This article is a PNAS direct submission.

Abbreviations: OSN, olfactory sensory neuron; OE, olfactory epithelium; OB, olfactory bulb; OR, odorant receptor; AC3, adenylyl cyclase type 3; P*n*, postnatal day *n*; E*n*, embryonic day *n*; GPCR, G protein-coupled receptor; tGFP, tauGFP.

†To whom correspondence should be addressed. E-mail: sjf24@columbia.edu.

This article contains supporting information online at www.pnas.org/cgi/content/full/0609215104/DC1.

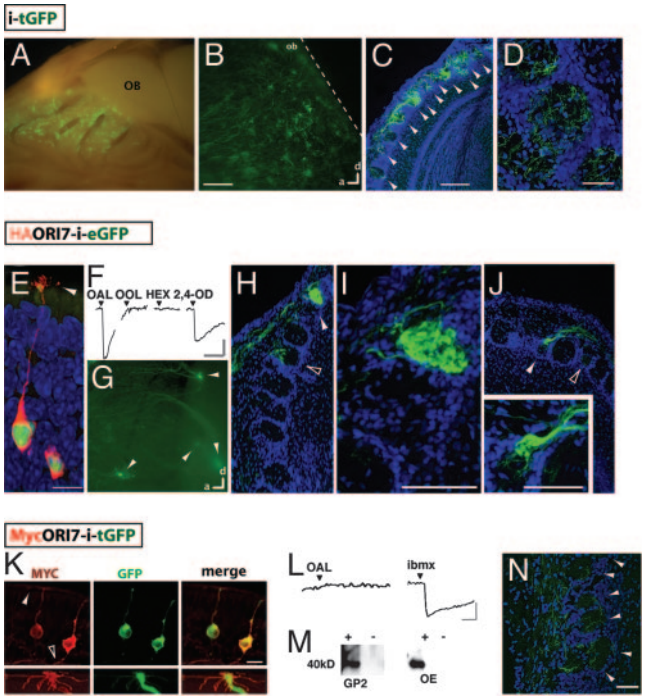

Fig. 1. Glomerular convergence of axons from OSNs expressing the functional ectopic rat ORI7. (*A–D*) Injection of a retroviral vector encoding tGFP following an internal ribosome entry site results in widespread ectopic expression. (*A*) Medial view of olfactory turbinates in a P21 mouse that had been injected at E11.5. Numerous GFP$^+$ clusters of cells (green) are apparent throughout the OE. (*B*) Whole-mount image of a P21 rat OB showing that numerous GFP$^+$ axons diffusely project to the OB but do not invade the cortex (dashed line). (Scale bar, 200 μm.) (*C*) Confocal projection of a 20-μm cryosection from a rat OB showing GFP$^+$ axons entering many glomeruli. TOTO3 (blue) labels all of the nuclei. Arrowheads indicate glomeruli. (Scale bar, 100 μm.) (*D*) Confocal projection of a 60-μm cryosection from a rat OB showing how these fibers enter and branch within glomeruli. (Scale bar, 25 μm.) (*E–J*) Ectopic expression of functional HA-ORI7 alters odorant responses and axonal projections. (*E*) As shown by immunohistochemistry, HA-ORI7 protein (red) localizes to OSN cell bodies, dendrites, and cilia (arrowhead) and overlaps with EGFP (green) in a P7 rat injected at E15. (Scale bar, 6.25 μm.) (*F*) Calcium imaging of dissociated GFP$^+$ OSNs from 3- to 4-week-old rats injected at E15. Two ORI7 agonists [octanal (OAL) and trans, trans2,4-octadienal (2,4-OD)] and two odorants known not to activate the receptor [octanol (OOL) and hexanal (HEX)] are selected as a diagnostic panel for ORI7 function. The correct response profile largely identifies ORI7 from the other ORs that also respond to OAL. All odorants were presented at 30 μM. (Vertical scale bar, 10% ΔF/F; horizontal scale bar, 2 min.) (*G*) Whole-mount image of a P21 rat injected at E15 with HA-ORI7 retroviral vector results in numerous GFP$^+$ axons converging at multiple locations in the OB. Arrowheads indicate four observable convergences. (*H–J*) Sections of OB from an infected P21 rat reveal HA-ORI7 axons converging in the OB. (*H*) A section of an OB from a 3-week-old rat injected with HA-ORI7 at E15 shows a heterogeneous glomerulus (open arrowhead) within 200 μm of a homogeneous glomerulus (white arrowhead). (*I*) Higher-magnification view of the homogeneous glomerulus shown in *H*. (Scale bar, 50 μm.) (*J*) Another example of axonal convergence. (*Inset*) A higher-magnification view of the glomerulus (white arrowhead) showing that many of the fibers have coalesced. Note that the fibers do not appear to fill the entire glomerulus. (Scale bar, 100 μm.) (*K–N*) Ectopic expression of Myc-I7 in OSNs (Myc-I7-i-tGFP). (*K*) (*Upper*) Myc-ORI7 (red) traffics to OSN cilia (white arrowhead) and axons (open arrowhead). OSNs coexpress tGFP (green). (Scale bar, 12.5 μm.) (*Lower*) A higher magnification of the dendrite of a transduced OSN (green) showing Myc immunoreactivity (red) in the cilia. (*L*) As indicated by calcium imaging, expression of Myc-ORI7 does not confer responsiveness to octanal (OAL) at 30 μM. However, the OSNs still respond to 3-isobutyl-1-methylxanthine (IBMX), indicating an intact transduction pathway. (Vertical scale bar, 10%ΔF/F; horizontal scale bar, 30 s.) (*M*) Western blots using the Myc antibody from the retrovirus-producing GP2 cell line and infected rat OE indicate the expression of a full-length Myc-ORI7 protein. (*N*) Ectopic expression of nonfunctional Myc-ORI7 in OSNs does not result in coalesced axons (green) in a P21 rat (compare to ectopic functional HA-ORI7 expression in *G–J*). (Scale bar, 120 μm.)

newborn OSNs were readily observed in the OB. After birth, a network of numerous tGFP+ axons covered the OB (Fig. 1*B*). These axons entered many glomeruli, where they branched (Fig. 1 *C* and *D*). In sum, we have taken advantage of the fact that retroviral vectors productively infect only dividing cells to develop a technique that allows us to ectopically express genes in newly born OSNs and to study OSN axon projections as they extend into the OB.

Ectopic Expression of ORI7 in Developing OSNs Induces Their Axons to Coalesce. Current models posit that OSN axonal identity is determined by OR expression. With the retrovirus, we could directly ask whether OR expression alone was sufficient to determine OSN axonal identity by forcing the precocious expression of an ectopic OR. Injection of a retroviral vector encoding an N-terminally tagged rat ORI7 construct (HA-ORI7) followed by IRES-EGFP resulted in mosaic expression throughout the OE. The OR protein was detected by using the HA epitope tag in the cell body, dendrites, and cilia of OSNs (Fig. 1*E*), indicating proper OR trafficking (17, 18). The OSNs ectopically expressing HA-ORI7 appeared phenotypically normal, expressing the various cell-type-specific markers, including OMP and endogenous ORs (data not shown). Overall, ectopic expression resulted in expression in many more neurons (>2-fold) than is typically seen for endogenous ORs.

ORI7 is activated by octanal and structurally related ligands (19). We therefore asked whether exogenous HA-ORI7 was sufficient to alter the odorant response properties of OSNs in which it was ectopically expressed. Calcium imaging with a diagnostic panel of four ligands was used to distinguish ORI7 from the ≈50 other ORs thought to be sensitive to octanal (Fig. 1*F*) (19). One hundred percent of octanal-responsive GFP$^+$ OSNs displayed the expected ORI7 profile, thus confirming that HA-ORI7 is functional ($n = 6$). For comparison, similar to our previous study (20), only 13% of the octanal-responsive GFP$^-$ OSNs possessed an ORI7-like profile ($n = 15$). From the calcium imaging experiments, we conclude that the exogenous HA-ORI7 alters the odorant response properties of OSNs in an expected manner.

We next tested whether the exogenous OR protein was sufficient to alter axonal identity by examining the projection of transduced OSNs. Whole-mount images and serial sections of P21 rat OBs (infected at E15) revealed that ectopic HA-ORI7 expression resulted in the convergence of axons into multiple distinct glomeruli throughout the OB (Fig. 1*G*). Such coalescence was never observed in tGFP controls (Fig. 1 *B* and *D*). We noted a large variation in the number, position, and size of the ectopic glomeruli between individuals [Fig. 1 *G–J* and supporting information (SI) Fig. 4]. However, despite the variation in position, convergence of OSN axons was observed in all animals with broad infections ($n = 50$; covering >20% of the visible OE area in bisected nasal cavity), ranging from two to eight glomeruli per half-bulb. Among them, we observed homogenous (Fig. 1*I*), partially coalesced (Fig. 1 *H* and *J*, open arrowheads), and compartmentalized glomeruli (Fig. 1*J Inset*; SI Fig. 4 *B* and *C*) with a relative ratio of 2:5:3. Animals with less robust infection were not analyzed, because it had been reported that a minimum number of OSN axons are needed to support a glomerulus (21). Overall, these data clearly demonstrated that the expression of a functional OR was sufficient to induce axonal sorting into glomeruli.

ORI7 Function Correlates with the Axonal Guidance Phenotype. Expression of an ectopic OR both altered odorant response profiles and induced coalescence of OSN axons, raising the possibility that OR function, not just expression, was important. Serendipitously, we found that a different N terminus modification, the addition of a Myc tag, disrupted ORI7 function, allowing us to

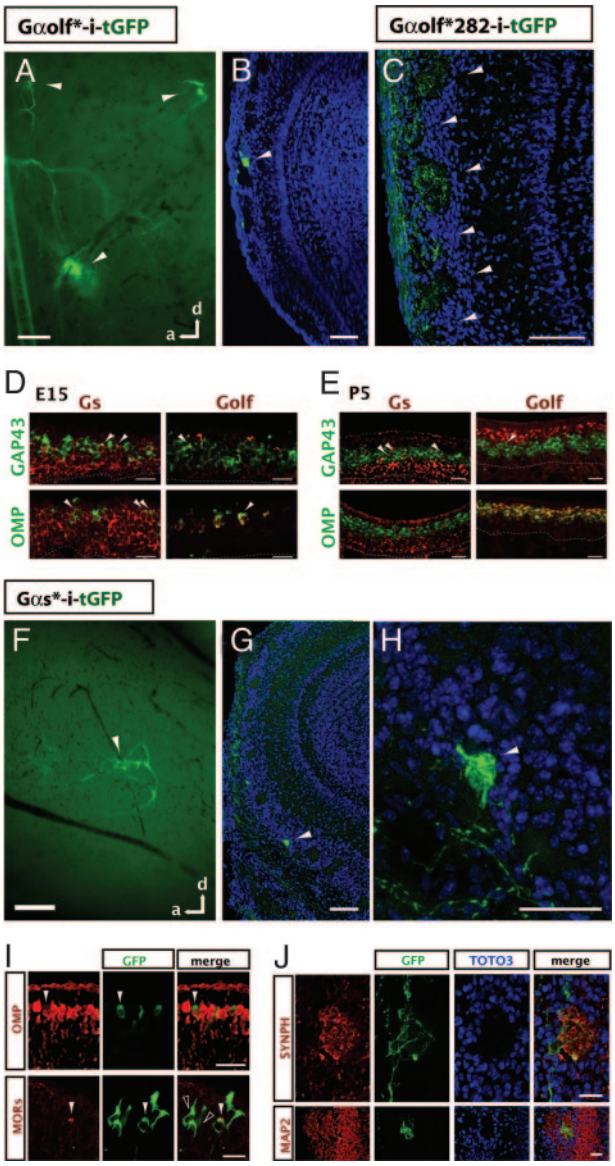

Fig. 2. Unique axonal identities encoded by OSN signal transduction. (*A* and *B*) Ectopic expression of a constitutively active Gαolf mutant (Gαolf*-i-tGFP) induces axonal sorting. (*A*) A whole-mount sagittal view of the OB from a P7 rat injected with a Gαolf* retroviral vector at E15. One large tGFP convergence, as well as two smaller ones, is visible (arrowheads). (Scale bar, 100 μm.) (*B*) A 20-μm cryosection of a different OB reveals axons from OSNs expressing Gαolf* coalescing into a glomerulus (arrowhead) in a P7 rat. TOTO3 (blue) labels all of the nuclei in the OB. (Scale bar, 100 μm.) (*C*) Axons from OSNs expressing a mutant of Gαolf* with reduced activity (Gαolf*282-i-tGFP) no longer sort into glomeruli. The resulting pattern is indistinguishable from tGFP controls (Fig. 1*D*). (Scale bar, 100 μm.) (*D* and *E*) Two-color *in situ* hybridization (ISH) reveals developmental dynamics of stimulatory Gα subunit expression in the OE. (*D*) Two-color ISH of Gαs (*Left*) or Gαolf (*Right*; both red) at E15 with two markers for OSN maturation (GAP43 on top and OMP on bottom; both green). Gαs expression is more widespread than Gαolf in both immature cells (GAP43$^+$; arrowheads) and mature cells (OMP$^+$; arrowheads). (*E*) Two-color ISH at P5. At this stage, Gαs is more restricted to the basal OE but can still be found expressed in a few immature OSNs (arrowheads). Gαs is absent from the mature population. Conversely, Gαolf expression is largely restricted to the apical OE, where it completely overlaps with OMP, the marker for mature OSNs. Dashed lines indicate the basal lamina. (Scale bar, 25 μm.) (*F–J*) Ectopic expression of constitutively active Gαs mutant (Gαs*-i-tGFP). (*F*) Similar to Gαolf*, ectopic expression of Gαs* also results in axonal convergence (arrowhead) in the whole-mount OB of a P7 rat that was infected at E15. (Scale bar, 200 μm.) (*G*) Axons from OSNs ectopically expressing Gαs* sort and coalesce into a glomerulus (arrowhead). (Scale bar, 100 μm.) (*H*) A magnified view of the glomerulus in *G* (arrowhead). (Scale bar, 50 μm.) (*I*) (*Upper*) Expression of Gαs* (indicated by GFP, green) does not inhibit OSN maturation as assayed by OMP expression (red, arrowheads). (*Lower*) Expression of Gαs* also does not inhibit endogenous OR expression, as seen by immunostaining with anti-GFP (green) and a mixture of antibodies for OR37 and OR256–17 (red) in a P7 mouse. Double-labeled cell is indicated by white arrowhead. Importantly, not all GFP+ OSNs express the same OR. Open arrowheads indicate OSNs not expressing either OR37 or OR256–17. (Scale bar, 25 μm.) (*J*) (*Upper*) The axon terminals of OSNs expressing Gαs* (labeled by GFP, green) are enriched for the synaptic marker synaptophysin (Synph; red) even in heterogeneous glomeruli. (*Lower*) The ectopic Gαs* glomeruli are innervated by the dendrites of MAP^{2+} bulbar neurons (red). (Scale bar, 25 μm.)

test this proposition. Despite proper trafficking to OSN cilia (Fig. 1*K*), Myc-ORI7 expression in OSNs did not confer responsiveness to OAL (0/5 IBMX-responsive GFP+ OSNs; Fig. 1*L*). Western blots showed that the loss of function did not result from the production of a truncated OR protein (Fig. 1*M*). Calcium imaging experiments further indicated that the Myc-ORI7-expressing OSNs were still physiologically functional (Fig. 1*L*). However, the nonfunctional Myc-ORI7 protein in OSN axons (Fig. 1*K*, open arrowheads) failed to cause these axons to coalesce (Fig. 1*N*). Instead, the axons entered many glomeruli in a manner indistinguishable from tGFP controls (compare Fig. 1 *D* and *N*). These results suggest that OR function is necessary for inducing axonal convergence.

Ectopic Activation of G Protein Signaling Results in Axonal Coalescence. Based on our tagged ORI7 experiments, we hypothesized that activation of the transduction cascade encodes critical information about the OR expressed by a given OSN. We therefore tested the influence of downstream signaling by directly activating transduction among a subset of OSNs. OR-induced activation of Gαolf stimulates the production of the second-messenger cAMP by AC3 (13) and is required for odorant responses in OSNs (9). We therefore expressed a mutant of Gαolf (Q214L) that possesses reduced GTPase activity, thus increasing its basal level of activity (Gαolf*; ref. 22). We first determined that Gαolf* could productively couple to ORs by using a defined OR in a heterologous expression assay. Furthermore, the elevated basal level was not saturating, and odorant responsiveness appeared similar to that of Gαs (SI Fig. 5).

Although the cell bodies of OSNs ectopically expressing Gαolf* were distributed throughout the OE in a manner similar to that for tGFP (Fig. 1*A*), remarkably, their axons coalesced into glomeruli in the OB (Fig. 2 *A* and *B*). The axonal sorting phenotype was very robust and was observed in all mice and rats examined (n = 21) ranging in age from P3 to P21. Like with HA-I7, the widespread expression of Gαolf* across the zones in the OE resulted in the formation of numerous ectopic glomeruli (2–10 per half-bulb). From these experiments, we conclude that increased Gαolf signaling is sufficient to create an axonal phenotype resulting in axonal sorting and coalescence into glomeruli.

As a negative control, we expressed an additional mutant of Gαolf* that decreases the G protein's overall GTP affinity (Gαolf-Q214L/D282N), thus reducing its basal level of activity (SI Fig. 5*B*; ref. 22). We found Gαolf*282 coupled very poorly to heterologously expressed ORs (SI Fig. 5*B*). More critically, when expressed in developing OSNs *in vivo*, the double mutant (Gαolf*282) failed to induce axonal coalescence (Fig. 2*C*). Indeed, axons from OSNs expressing Gαolf*282 looked indistinguishable from axons expressing tGFP alone (Fig. 1 *B–D*). From these data, we conclude that Gαolf must be sufficiently active to induce OSN axons to sort into glomeruli.

NEUROSCIENCE

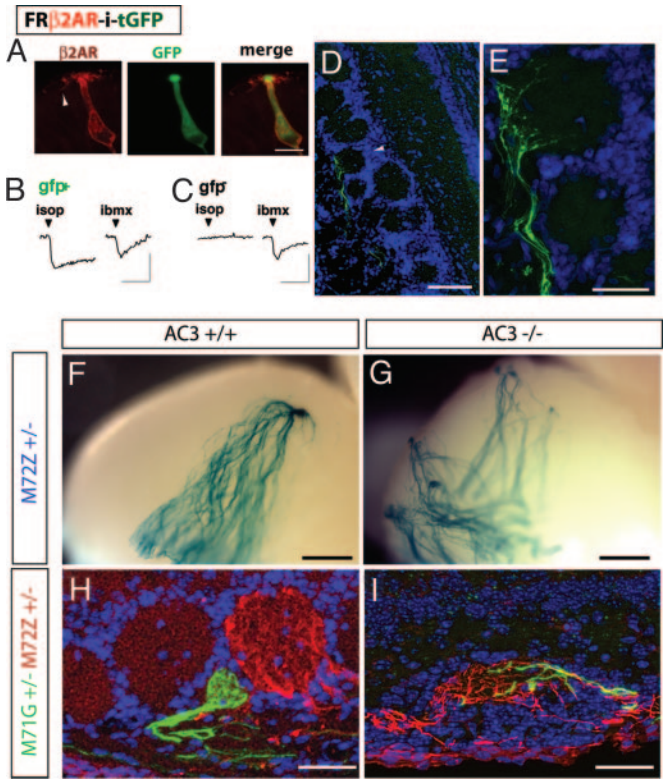

Fig. 3. Activation of cAMP pathway underlies GPCR induction of axonal coalescence. (*A–E*) Ectopic expression of functional human β2AR in OSNs (FR-β2AR-i-tGFP) results in axonal convergence. (*A*) Immunohistochemical staining reveals that β2AR protein (red) traffics to OSN cilia in a P7 mouse OE injected with a retroviral vector at E13. (Scale bar, 10 μm.) (*B*) A GFP$^+$ OSN dissociated from a P21 rat infected at E15 responds to 10 μM isoproterenol. (*C*) GFP$^-$ OSNs in the same field of cells are not activated. (Vertical scale bar, 10%ΔF/F; horizontal scale bar, 2 min.) (*D* and *E*) Axons (green) of OSNs ectopically expressing β2AR converge in the OB but do not fully enter a glomerulus (white arrowhead) in a P21 rat. TOTO3 (blue) labels all of the nuclei in the OB. [Scale bar: *D*, 100 μm; *E* (enlarged view of *D*), 25 μm.] (*F–I*) Lack of AC3 activity perturbed axonal sorting. M71G and M72Z mice are crossed with AC3 knockout mice to generate compound mutants. At P20, M72Z axon projection in the bulb is observed in the whole-mount stained with X-Gal. M71G and M72Z axonal innervation patterns in glomeruli are studied by immunohistochemistry. (*F*) Convergence of the M72 axons into a single glomerulus in the posterior medial half-bulb of AC3 wild-type mice. (*G*) Highly perturbed projection of M72 axons in an AC3$^{-/-}$ littermate. (*H*) In the AC3$^{+/+}$ background, M71G (green) and M72Z (red) axons converge into distinct glomeruli within close proximity of one another. (*I*) In the AC3$^{-/-}$ background, M71G and M72Z axons intermingle within the same glomerulus. (Scale bar, *A* and *B*, 500 μm; *C* and *D*, 25 μm.)

Embryonic Activation of Gαs Induces Axonal Coalescence. Although the targeted deletion of Gαolf resulted in anosmia and significantly reduced peripheral odorant responses, the formation of the glomeruli for OR P2 appeared unperturbed at P0 (9). This suggests that, at least in embryos, Gαolf is not necessary for the convergence of some populations of OSN axons. However, it remained possible that ORs still coupled to another G protein in neonates, particularly the highly homologous stimulatory Gαs.

We therefore examined the expression patterns of Gαs and Gαolf at E15 and P5 (Fig. 2 *D* and *E*, respectively). At E15, when OSN axonal sorting begins, we found widespread expression of Gαs throughout the OE. Gαs was expressed not only in progenitor cells (data not shown) but also in GAP43$^+$immature OSNs and OMP$^+$ mature OSNs. Gαolf expression, on the other hand, was very sparse and largely restricted to the few mature OSNs present at this point (Fig. 2*D*). In contrast, at P5, when many glomeruli have emerged, Gαs was still highly expressed by progenitor cells but was now only weakly expressed by some immature neurons and not detected in mature OSNs. Gαolf expression was largely absent from immature OSNs, being expressed almost exclusively by OMP$^+$ neurons (Fig. 2*E*). In summation, our results suggest Gαs may partner with ORs in embryonic and immature OSNs during the process of axon extension and convergence, whereas Gαolf is expressed in mature OSNs whose main function is odor-evoked transduction (summarized in SI Fig. 6).

We thus investigated whether Gαs activation underlies axon sorting. Unfortunately, disruption of the widely expressed Gαs gene results in embryonic lethality by E10.5 (23), thwarting loss-of-function studies. We therefore took an alternative approach to testing the role of Gαs by using our gain-of-function assay. We expressed a mutant, Gαs-Q227L (Gαs*), which possesses increased basal signaling (SI Fig. 5; ref. 22). As was the case with Gαolf*, Gαs* productively coupled to heterologously expressed ORs where, despite having elevated activity, the odorant-induced dose–response curves had similar saturation kinetics as wild-type Gαs (SI Fig. 5).

Ectopic expression of Gαs* in developing OSNs was sufficient to induce the coalescence of their axons in every animal examined, including both mice and rats ($n = 22$; Fig. 2 *F–H*). We found that OSNs ectopically expressing Gαs* still expressed ORs normally. Importantly, staining with OR-specific antibodies revealed that not all of the Gαs*-positive OSNs expressed the same OR (Fig. 2*I*), thus indicating that elevated Gαs activity does not promote the expression of a particular OR. Many of these OSNs appeared to mature fully (Fig. 2*I Upper*). Furthermore, the sites of convergence were enriched with markers of synapse formation and contained the dendrites of projection neurons (Fig. 2*J*), suggesting they are functional glomeruli. Our results support the view that the activity of stimulatory Gα subunits underlies OSN axonal sorting and subsequent coalescence into glomeruli.

Functional Nonolfactory G Protein-Coupled Receptor (GPCR) Induces Axonal Coalescence. Our results pointed to a model where OR activation of a stimulatory G protein cascade induced axonal sorting. One prediction of this model is that nonolfactory GPCRs should induce the axonal convergence if they can activate Gαs/Gαolf signaling in OSNs. It was shown that targeted replacement of the OR-M71 coding region with the mouse β2AR resulted in the creation of novel glomeruli (24). However, that study did not examine whether β2AR was functionally coupled to OSN transduction. We ectopically expressed a flag-rho tagged human β2AR by using a retroviral vector and found that, like HA-ORI7 and Myc-ORI7, ectopic β2AR was localized in OSN cilia and axons (Fig. 3*A*). When stimulated with the β2AR agonist isoproterenol, 5/5 (100%) OSNs expressing ectopic β2AR responded in calcium imaging (Fig. 3*B*). In contrast, virtually none of the GFP$^-$ [yet 3-isobutyl-1-methylxanthine (IBMX)-responsive] OSNs (3/144; 2%) from the same field of cells responded to isoproterenol (Fig. 3*C*). As predicted, the ectopic expression of β2AR resulted in OSN axons coalescing into multiple glomeruli throughout the OB (Fig. 3 *D* and *E*), although we noted that, in many cases, the axons often did not fully enter the glomerulus (i.e., Fig. 3*E*). It is unclear why β2AR was less effective than HA-I7 in inducing axonal coalescence; it may reflect differences in basal signaling, coupling efficiency, or protein levels. Conversely, when we ectopically expressed V1Rb2, a GPCR thought not to couple to Gαs but rather to Gαo, we failed to detect either calcium responses to its ligand 2-heptanone (25) or coalesced axons (data not shown).

Disruption of the cAMP Pathway Perturbs Axonal Projection. We hypothesized that a critical outcome of Gαs signaling in the OSNs contributing to axonal sorting was the stimulation of cAMP pro-

duction. We therefore decided to analyze mice where the function of AC3 was genetically disrupted. AC3 is required for odorant transduction and is activated by both Gαolf and Gαs (13). In the $AC3^{-/-}$ mice, odor-evoked electrical activity was completely abolished, and forskolin-induced cAMP generation was greatly reduced. Moreover, glomerular structures in the OB of $AC3^{-/-}$ mice have gross morphological defects (14). By crossing into an $AC3^{-/-}$ background gene-targeted mice that coexpresses the marker tauLacZ with the OR M72 (M72Z; ref. 8), we examined the contribution of cAMP signaling in the precise projection of M72 axons. In $AC3^{+/+}$ mice at P20, M72 axons normally converged into a single glomerulus in either the medial or lateral posterior half-bulb (Fig. 3*F*; ref. 12). In stark contrast, in the $AC3^{-/-}$ mice background, M72 axonal projection was highly disrupted with M72 axons found in numerous atypical locations in both the anterior and posterior OB ($n = 3$ OBs, Fig. 3*G*).

The disorganized projection pattern suggested that M72 axons had lost their unique identity in the $AC3^{-/-}$ background. We thus examined another hallmark of M72Z axons, their ability to sort from the axons of OSNS expressing M71, a highly homologous OR (10). By using mice with M71 and M72 receptors differentially marked [M71-IRES-tGFP (M71G) and M72Z], in the $AC3^{+/+}$ background, we observed, as expected (10), that these two populations sorted from each other into homogenous populations (Fig. 3*H*). However, in an $AC3^{-/-}$ background, M71 and M72 axons now intermingled (Fig. 3*I*). Mixed M71/M72 glomeruli were found in 83% of the three broad projection regions analyzed per OB (anterior, posterior lateral, and posterior medial; $n = 12$ OB projection regions) in the $AC3^{-/-}$ mice. These data strongly implicate cAMP signaling as a requirement for the establishment of a unique OSN axonal identity.

Discussion

The key event in the development of ordered connections between the OE and the OB is the coalescence of >1,000 populations of axons into homogenous glomeruli. This remarkable sorting process is guided by the expression of a specific OR that appears to serve a double duty, conferring ligand recognition in the periphery and axonal identity in the OB. Whether the OR itself is both necessary and sufficient and what molecular steps underpin the OR's function in guidance have remained open questions since the initial observation (1).

We have used a retroviral-based technique to manipulate expression of the key genes in the pathway coupling the OR to cellular activity to explore the axonal sorting mechanism. The technique offers a complementary approach to the use of transgenic mice in that gene expression is mosaic, avoids potential issues of lethality, and provides temporal and spatial control. In keeping with previous work, we found that ectopic expression of only functional receptors drove OSN axons to coalesce in the OB. Additionally, we have demonstrated that a feature universal to GPCRs, downstream coupling to intracellular G protein cascades, functions in axonal sorting. Last, through the examination of gene-targeted animals, we have linked a requirement for cAMP-dependent signaling pathways to the formation of glomeruli.

Formation of Glomeruli. A hallmark of a mature glomerulus is the homogeneous innervation by axons from cells expressing the same OR (2) and largely stereotyped positioning in the OB. Although many factors have been shown to influence the positions of glomeruli (11), the sorting of axons and their coalescence into homogenous fascicles seemed to have a single determinant, the ORs. There is strong evidence that OR amino acid sequence, level of OR protein expression, and timing of OR expression are all important determinants of sorting (10). We now suggest that receptor activation and downstream signaling by stimulatory Gα subunits are also critical determinants of axonal coalescence into glomeruli.

Based on our expression studies, we find that Gαs is expressed at the right time and place to participate in OSN axon guidance. Furthermore, we demonstrate that activation of the G protein cascade is sufficient to induce axonal sorting. We observe OSN axons sorting apparently independently of the expression of a specific OR, relying instead on G protein activity. Although our interpretation differs, our finding is consistent with those of Feinstein and Mombaerts (10), who demonstrated that the Gαs-coupled β2-adrenergic receptor sufficiently substituted for an OR, but a presumably Gαo-coupled Vomeronasal receptor (V1Rb2) was largely insufficient to engender glomerular formation (24). Last, we identify the generation of cAMP as a key player in conferring OSN axonal identity. Examination of the OBs of $AC3^{-/-}$ mice, and in particular of the fate of OSN populations expressing two closely related ORs (M71 and M72), further underscores that cAMP is a key player in the axonal sorting process.

Sorting Machinery. Although the downstream targets of the G protein signaling remain unknown, several models can be envisioned (SI Fig. 6). There are several examples of GPCR signaling affecting growth cone turning through alterations of cAMP, cGMP, and/or Ca^{2+} levels (26, 27). Alternatively, cAMP and/or Ca^{2+}-dependent gene transcription may indirectly control sorting through the regulation of guidance genes (SI Fig. 6*D*). cAMP and Ca^{2+} are both well established potent modulators of gene expression for numerous genes in diverse pathways (28). The expression of ORs before OSN maturation and the coexpression of Gαs with ORs in the embryonic OE are consistent with such a function. These models are consistent with the finding that modulation of PKA and CREB activity alters gene transcription profiles and glomerular position (29). However, ectopic expression of an active PKA mutant in a mosaic of OSNs by using a retroviral vector was insufficient to promote coalescence (A.T.C., unpublished data). Thus, although G protein stimulation of cAMP is clearly involved in axonal coalescence, there are likely multiple downstream targets of this pathway.

Establishing Axon Identity Through an OR Code. It remains challenging to explain how G protein signaling from >1,000 ORs results in such apparently precise wiring in the adult. For example, ORs M71 and M72 that differ by only 11 amino acids (96% identity) and have overlapping response profiles are able to sort into two distinct glomeruli in close proximity (10). Because it is unlikely there exist >1,000 ligands in the OB acting as guidance cues for the >1,000 ORs, activation of the ORs had not previously been considered necessary for their role in axon guidance. However, we show that, without AC3 activity, OSN populations are no longer able to maintain their individuality.

It has been suggested that the ORs function in axon guidance by homotypic interactions (10). However, if OR interactions alone were both necessary and sufficient to instruct axonal sorting (10), it is difficult to imagine how the ectopic constitutively active Gαolf or Gαs could induce axons to coalesce. One would have to envision the unlikely scenario that increasing the basal level of G protein signaling causes either up-regulation of a specific OR in these cells or the selective survival of a single population of OSNs. Based on our immunohistochemistry and OR *in situ* experiments (A.T.C. and C.E.L.P., unpublished observations), this seems highly unlikely.

An alternative possibility is that homotypic interactions modulate Gαs activity, thus providing a link between interacting ORs and intracellular pathways. Ectopic activation of Gαs could have allowed OSN axons expressing ORs with only weak homotypic interactions to remain associated. Conversely, disruption of cAMP signaling could serve to destabilize strong homotypic

interactions. Last, in the absence of OR-mediated homotypic interactions, differences in ligand-independent basal signaling could be sufficient to generate OR-specific signatures, because many GPCRs are believed to have high levels of constitutive signaling (30).

Conclusions

Although the notion that the ORs themselves provide axonal identity is very appealing, no mechanism by which the receptors could perform this function has been demonstrated. Despite data supporting activity-independent sorting (6–9), our results and those of others challenge this notion (12–15). These discrepancies can be reconciled by a model in which the informative role of activity begins with the G protein/cAMP cascade. The mechanisms by which specific ORs activate the G protein cascade and the targets of the signaling remain to be determined.

Materials and Methods

Animals. Timed pregnant Swiss–Webster mice and Sprague–Dawley rats were from Taconic Farms (Germantown, NY). $AC3^{-/-}$ mice were from D. R. Storm (13). M71-IRES-tGFP and M72-IRES-taulacZ mice were from P. Feinstein and P. Mombaerts (10).

Ultrasound-Guided Injection. This method was adapted from Gaiano *et al.* (16). Embryos were imaged by using a Paradigm P45 Ultrasonic workstation equipped with a 50-MHz transducer. The OE was injected using a Drummond PCR micropipette with a 30° beveled tip and a 20- to 40-mm opening, controlled by a Picospritzer III (General Valve) with pressures of 6–9 psi (1 psi = 6.89 kPa) and 50- to 100-ms durations.

Viral Constructs. All viruses were made using the Pantropic Retroviral Expression System (Clontech, Mountain View, CA) with the pLNCX2 vector according to the manufacturer's protocols. For construct details, see *SI Text*.

***In Situ* Hybridization and Immunostaining.** Two-color fluorescent *in situ* hybridization was performed as described in Ishii *et al.* (31). Immunostaining was performed as reported (12). For probe sequences and antibody specifications, see *SI Text*.

Functional Assays. Calcium imaging was performed as reported (20). Dual luciferase assays were performed per the manufacturer's instructions (Promega, Madison, WI). For details, see *SI Text*.

We thank members of the S.F. laboratory for comments; P. Feinstein (The Rockefeller University, New York, NY) and M. Rogers for comments and materials; and C. Zhang (Columbia University), T. Ishii (The Rockefeller University), F. Margolis (University of Maryland, Baltimore, MD), K. Touhara (University of Tokyo, Tokyo, Japan), H. Breer (University of Hohenheim, Stuttgart, Germany), and D. Storm (University of Washington, Seattle, WA) for materials. This work was supported by the National Institute on Deafness and Other Communication Disorders.

1. Mombaerts P, Wang F, Dulac C, Chao SK, Nemes A, Mendelsohn M, Edmondson J, Axel R (1996) *Cell* 87:675–686.
2. Treloar HB, Purcell AL, Greer CA (1999) *J Comp Neurol* 413:289–304.
3. Buck L, Axel R (1991) *Cell* 65:175–187.
4. Zhang X, Firestein S (2002) *Nat Neurosci* 5:124–133.
5. Malnic B, Hirono J, Sato T, Buck LB (1999) *Cell* 96:713–723.
6. Baker H, Cummings DM, Munger SD, Margolis JW, Franzen L, Reed RR, Margolis FL (1999) *J Neurosci* 19:9313–9321.
7. Lin DM, Wang F, Lowe G, Gold GH, Axel R, Ngai J, Brunet L (2000) *Neuron* 26:69–80.
8. Zheng C, Feinstein P, Bozza T, Rodriguez I, Mombaerts P (2000) *Neuron* 26:81–89.
9. Belluscio L, Gold GH, Nemes A, Axel R (1998) *Neuron* 20:69–81.
10. Feinstein P, Mombaerts P (2004) *Cell* 117:817–831.
11. Mombaerts P (2006) *Annu Rev Cell Dev Biol* 22:713–737.
12. Zou DJ, Feinstein P, Rivers AL, Mathews GA, Kim A, Greer CA, Mombaerts P, Firestein S (2004) *Science* 304:1976–1979.
13. Wong ST, Trinh K, Hacker B, Chan GC, Lowe G, Gaggar A, Xia Z, Gold GH, Storm DR (2000) *Neuron* 27:487–497.
14. Trinh K, Storm DR (2003) *Nat Neurosci* 6:519–525.
15. Yu CR, Power J, Barnea G, O'Donnell S, Brown HE, Osborne J, Axel R, Gogos JA (2004) *Neuron* 42:553–566.
16. Gaiano N, Kohtz JD, Turnbull DH, Fishell G (1999) *Nat Neurosci* 2:812–819.
17. Barnea G, O'Donnell S, Mancia F, Sun X, Nemes A, Mendelsohn M, Axel R (2004) *Science* 304:1468.
18. Strotmann J, Levai O, Fleischer J, Schwarzenbacher K, Breer H (2004) *J Neurosci* 24:7754–7761.
19. Araneda RC, Kini AD, Firestein S (2000) *Nat Neurosci* 3:1248–1255.
20. Araneda RC, Peterlin Z, Zhang X, Chesler A, Firestein S (2004) *J Physiol* (*London*) 555:743–756.
21. Ebrahimi FA, Chess A (2000) *Curr Biol* 10:219–222.
22. Yu B, Simon MI (1998) *J Biol Chem* 273:30183–30188.
23. Yu S, Yu D, Lee E, Eckhaus M, Lee R, Corria Z, Accili D, Westphal H, Weinstein LS (1998) *Proc Natl Acad Sci USA* 95:8715–8720.
24. Feinstein P, Bozza T, Rodriguez I, Vassalli A, Mombaerts P (2004) *Cell* 117:833–846.
25. Boschat C, Pelofi C, Randin O, Roppolo D, Luscher C, Broillet MC, Rodriguez I (2002) *Nat Neurosci* 12:1261–1262.
26. Nishiyama M, Hoshino A, Tsai L, Henley JR, Goshima Y, Tessier-Lavigne M, Poo MM, Hong K (2003) *Nature* 423:990–995.
27. Kafitz KW, Leinders-Zufall T, Zufall F, Greer CA (2000) *NeuroReport* 11:677–681.
28. West AE, Chen WG, Dalva MB, Dolmetsch RE, Kornhauser JM, Shaywitz AJ, Takasu MA, Tao X, Greenberg ME (2001) *Proc Natl Acad Sci USA* 98:11024–11031.
29. Imai T, Suzuki M, Sakano H (2006) *Science* 314:657–661.
30. Bond RA, Ijzerman AP (2006) *Trends Pharmacol Sci* 27:92–96.
31. Ishii T, Omura M, Mombaerts P (2004) *J Neurocytol* 33:657–669.